Desalination and Water Treatment
www.deswater.com
doi: 10.1080/19443994.2013.822324

52 (2014) 2282–2292
February

Taylor & Francis
Taylor & Francis Group

Removal of phosphorus ions from aqueous solutions using manganese-oxide-coated sand and brick

N. Boujelben[a,*], F. Bouhamed[a], Z. Elouear[a], J. Bouzid[a], Mongi Feki[b]

[a]*Laboratoire Eau Energie et Environnement, Département de Génie Géologique, Ecole Nationale d'Ingénieurs de Sfax, BP 3038 Sfax, Tunisia*
Tel. +216 26872754; Fax: +216 74665190; email: nesrine.boujelben@tunet.tn
[b]*Unité de Chimie Industrielle I, Ecole Nationale d'Ingénieurs de Sfax, BP W 3038 Sfax, Tunisia*

Received 15 December 2012; Accepted 11 June 2013

ABSTRACT

Manganese-oxide-coated sand (MOCS) and manganese-oxide-coated crushed brick (MOCB) were characterized and employed for the removal of phosphorus ions (PO_4^{3-}) from aqueous solution. Scanning electron microscope (SEM), FTIR, X-ray diffraction spectrum (XRD), and BET analyses were used to study the surface properties of the sorbents. Sorption of PO_4^{3-} from aqueous solutions was investigated by batch experiments. The estimated optimum pH of phosphorus ions retention for the considered sorbents was 5. Both Freundlich and Langmuir isotherms may reasonably explain adsorption of phosphorus ions. The adsorption capacities of coated sorbents obtained at pH 5 and 20°C were 1.96 and 2.08 mg/g for MOCS and MOCB, respectively. The sorption kinetics were tested for pseudo-first order and pseudo-second order reactions as well as for intraparticle diffusion model and the rate constants of the three kinetic models were calculated. The best correlation coefficients were obtained using the pseudo-second-order kinetic model, indicating that PO_4^{3-} uptake process followed the pseudo-second order rate expression. Results from this study suggest that manganese-oxide-coated sorbent is potentially suitable to remove PO_4^{3-} from water.

Keywords: Phosphate ions; Sorption; Manganese oxide; Kinetic modeling; Thermodynamic parameters

1. Introduction

Phosphorous is the key nutrient for the growth of algal and other biological organisms, which in excess causes eutrophication of water bodies. The presence of phosphate industry in Sfax has led to a major problem of water pollution. For this reason, it becomes necessary to evaluate the capacities of some low-cost sorbents to eliminate phosphate ions from water. In this respect, several methods have been developed, among which chemical precipitation (with aluminum, iron, and calcium salts), biological processes that rely on biomass growth (bacteria, algae, and plants) or intracellular bacterial polyphosphate

*Corresponding author.

Presented at the 6th International Conference on Water Resources in Mediterranean Basin (WATMED6), 10–12 October 2012, Sousse, Tunisia

accumulation [1] and sorption (natural apatite, activated carbon, etc.) [2]. The later method would be comparatively more useful and economical than the others for this aim. Therefore, in recent years, considerable attention has been paid, based on economical and environmental concerns, to the investigation of different types of low-cost sorbents, such as alum sludge [3], red mud [4–6], fly ash [7,8], calcite [9], goetite [10], birnesite [11], apatite [12], zeolite (clinoptilolite) [13], and other waste materials [14,15]. Recent studies have shown that some filtration materials such as sand and burned clay coated with oxides (oxyhydroxides) of iron, aluminum or manganese, act as good and inexpensive sorbents [16,17] for both cations (Pb^{2+} [18,19]), Mn^{2+} [20]) and anions (PO_4^{3-} [16,21], AsO_4^{3-} [22]). Sorption on oxide coated sorbents can also allow retention of pollutants that are not removed by conventional treatment methods [23]. It is to note that investigations of these coated sorbents were based on the fact that elimination of iron and manganese ions from water is much highly improved by using old sand filters (which become coated during use) than new ones [22–26].

This study investigated the characteristics of two prepared coated sorbents: manganese-oxide-coated sand and manganese-oxide-coated crushed brick. The thermodynamic and kinetic study of PO_4^{3-} removal on these materials was also undertaken. The main objectives of this investigation were to examine quantitatively the effect of contact time, pH, and concentrations on PO_4^{3-} removal from aqueous solutions, as well as to check in detail the phosphorus removal kinetics.

2. Materials and methods

2.1. Sample preparation

Manganese-coated sorbents (sand and crushed brick) were prepared by impregnation process according to the procedure proposed by Bajpai and Chaudhuri (1999) [27].

Sand and crushed brick consist of grains with an average diameter of 0.6–0.7 and 0.9–1.2 mm, respectively. Specific gravity was 2.50 for sand and 2.39 g/cm^3 for crushed brick.

Before MnO_2 impregnation, the sorbents were submitted to acidic purification procedure (acid-wash with 1 M HCl) [28] in order to remove impurities that could affect sorption results.

Briefly, application of MnO_2 coating to the two sorbents was carried out by making $KMnO_4$ to react with hot $MnCl_2$ solution (48–50 °C), under alkaline conditions (pH 9), during 48 h. This procedure led to an uniform black coating.

2.2. Chemicals

Aqueous solutions containing phosphate ions (PO_4^{3-}) at various concentrations were prepared from sodium phosphate salt (NaH_2PO_4). The initial pH of the solutions was adjusted by adding either nitric acid or sodium hydroxide.

All chemicals used for the treatment of the different sorbents ($Fe(NO_3)_3{\cdot}9H_2O$, NaOH, HNO_3, HCl) and for sorption tests were of analytical quality. All solutions were prepared using deionized water.

Measurements of the initial and final pH of the phosphate ion solutions were carried out using a laboratory pH-meter (model pH 540 GLP) equipped with a combined glass electrode (SENTIX 41). A preliminary calibration is systematically carried out using suitable buffer solutions. UV-V spectrophotometer (HITACHI U 2000) was used to determine total phosphate concentration using the ascorbic acid method. The selected wavelength was 880 nm. Metallic species in the different solutions were analyzed by atomic absorption spectrophotometry (HITACHI Z-6100).

2.3. Sorbent characterization

Mineralogy of the manganese oxide coating was characterized using an X-ray diffractometer (Siemens, Germany) with CuKα radiation ($\lambda = 0.154$ nm). Scans were conducted from 0 to 60° at a rate of 2° per min.

The specific surface area (m^2/g) of each sorbent before and after coating was determined by the single-point BET (N_2) adsorption procedure.

The pH of zero point of charge (pHzpc) was determined by adding a known amount of adsorbent (0.1 g) to a series of bottles that contained 50 mL of deionized water. Before adding the adsorbent, the pH of each solution was adjusted to be in the range of 1.0–9.0 by the addition of either 0.1 M HNO_3 or 0.1 M NaOH. These bottles were then rotated for 1 h in a shaker, and pH values were measured at the end of the test. The pH of the suspensions was represented as a function of the initial pH of the solutions. The curve obtained theoretically crosses the bisector of axes at the point of zero charge [17]. A pH_{zpc} of 4.5 and 4.3 were obtained for MOCS and MOCB, respectively.

Morphology of sorbents before and after coating was obtained using a Philips XL 30 scanning electron microscope (SEM). Elemental spectra were obtained using energy dispersive X-ray spectroscopy during SEM observations.

2.4. Sorption experiments

Batch experiments included the kinetic studies, the pH effect and the sorption isotherms. Sorption experiments for the kinetic study were conducted as follows: 1 g of each coated sorbent was suspended in 25 ml solution containing 10 mg/l of phosphate ions. The solution pH was adjusted to 5 with 1 M HNO_3 and 1 M NaOH. The suspensions were stirred for different time intervals. To determine the influence of pH on phosphate ions sorption, experiments were performed at various initial pH, ranging between 2.3 and 10.8. Initial concentration of 10 mg/l of phosphate ions and 1 g of sorbent per 25 ml of solution were used. The suspensions were stirred for 2 h. Sorption isotherm studies were conducted by adding 5 g of each coated sorbent to a 250 ml solution containing various phosphate ion concentrations (5, 10, 15, 20, 25, 30 mg/l). The initial pH was maintained at 5, and the suspensions were stirred for 2 h. After filtration through a 0.45-membrane filter (MFS), the final concentrations of phosphate ions in the solutions were measured.

The Langmuir and Freundlich adsorption isotherm often used to describe the sorption of solutes from a liquid phase were applied to our experimental results. Linear form of the Langmuir equation can be expressed as follows:

$$\frac{C_e}{q_e} = \frac{1}{Q_0 b} + \frac{C_e}{Q_0} \quad (1)$$

where C_e is the equilibrium concentration (mg/L), q_e is the amount of phosphate ion sorbed at equilibrium, b is the sorption constant (L/mg) (at a given temperature) related to energy of sorption, and Q_0 is the maximum sorption capacity (mg/g).

The Freundlich isotherm is an empirical model that is based on adsorption on heterogeneous surface and active sites with different energy. The linearized Freundlich isotherm equation is represented by the following equation:

$$\ln Q = \ln K_f + \frac{1}{n} \ln C_e \quad (2)$$

where K_f and n are Freundlich constants indicating the adsorption capacity and the adsorption intensity, respectively. K_f and n are, respectively, determined from the intercept and slope of plotting ln Q vs. ln C_e.

In order to explain the effect of temperature on the adsorption thermodynamic parameters, Standard Gibbs free energy (ΔG°), Standard enthalpy (ΔH°), and Standard Entropy (ΔS°) were determined. The free energy change is obtained using the following relationship:

$$\Delta G^\circ = -RT \ln b \quad (3)$$

where R is the gas constant, b the equilibrium constant (obtained from Langmuir equation) and T is the temperature (K). Other thermodynamic parameters such as enthalpy change (ΔH°) and entropy change (ΔS°) are evaluated using Van't Hoff equation:

$$\ln b = \frac{\Delta S^\circ}{R} - \frac{\Delta H^\circ}{RT} \quad (4)$$

In order to determine the effect of temperature on sorption phenomenon, isotherms were established at 10, 20, and 40 °C.

2.5. Adsorption kinetics

Adsorption kinetic models are important in water treatment process design. In order to analyze the PO_4^{3-} adsorption kinetics on MOCS and MOCB, three kinetic models including the pseudo-first-order equation [29] and the pseudo-second-order equation [30] were applied to experimental data obtained previously for time-dependent PO_4^{3-} adsorption.

The pseudo-first-order kinetic model is given as:

$$\log(q_e - q_t) = \log q_e - [(K_1 t)/2.303] \quad (5)$$

The pseudo-second-order kinetic model is:

$$t/q_t = 1/(K_2 q_{e^2}) + t/q_e \quad (6)$$

In these equations, q_e and q_t are the amounts of solute adsorbed per mass unit of adsorbent at equilibrium and at any given time t, respectively (mg/g), K_1 the pseudo-first-order rate constant for the adsorption process (min^{-1}), K_2 the rate constant for the pseudo-second-order adsorption (g/mg min), $K_2 q_e^2 = h$ the initial sorption rate of the pseudo-second-order adsorption (mg/g min). A straight line of $\log(q_e - q_t)$ vs. t and t/q_t vs. t suggests the applicability of the kinetic models. The kinetic parameters can be determined from the slope and intercept of the plots.

3. Results and discussion

3.1. Sorbent characterization

3.1.1. SEM micrographs and EDAX spectra

SEM micrographs were taken to observe the morphology of the uncoated and the manganese-oxide-coated sand (MOCS) and crushed brick (MOCB). SEM

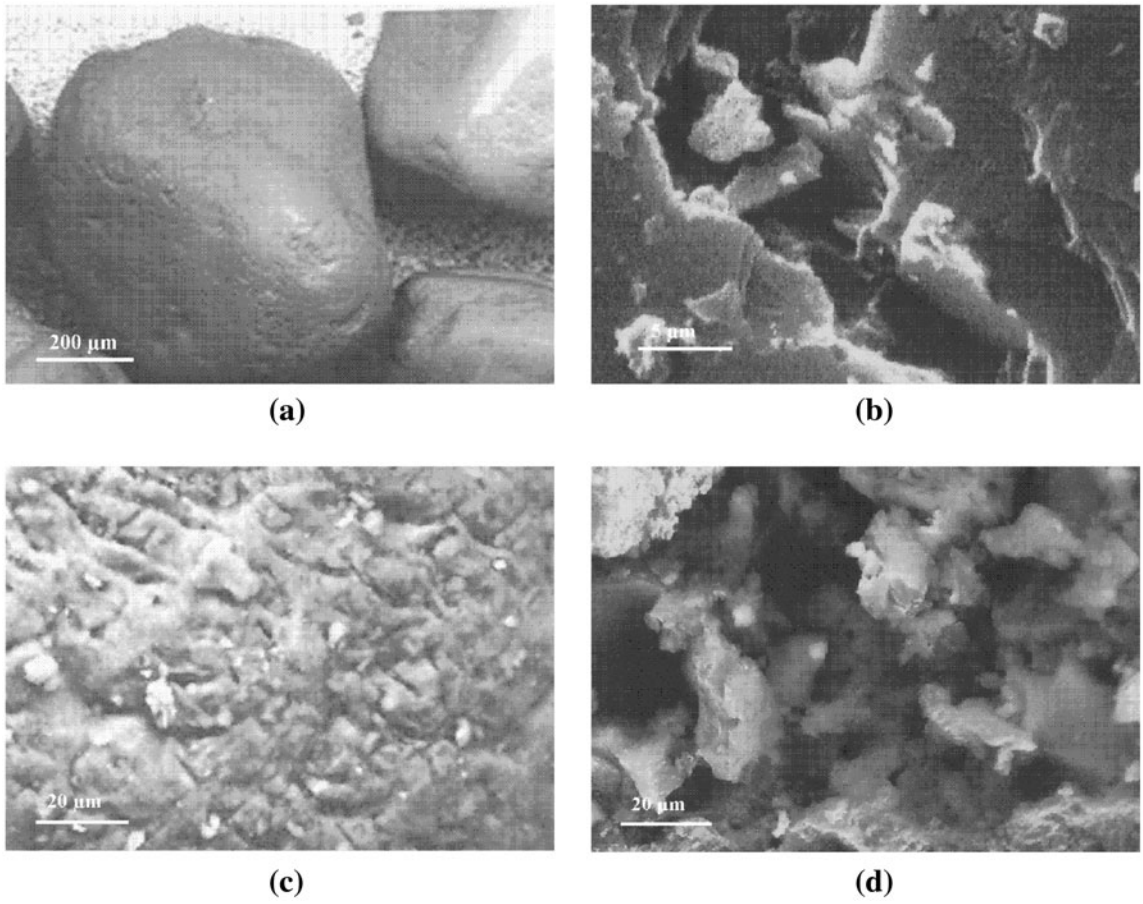

Fig. 1. SEM micrographs of samples: (a) US; (b) MOCS; (c) uncoated crushed brick and (d) MOCB.

images of acid-washed uncoated sand (US) and crushed brick (UB) (Fig. 1(a) and (c)) showed a very ordered silica crystals at the US surface and a regular aluminosilicate for UB. These two virgin materials had relatively uniform and smooth surfaces. Small cracks and light roughness could also be found on their surfaces. In return, manganese-oxide-coated surfaces (MOCS Fig. 1(b), MOCB Fig. 1(d)) were apparently occupied by newborn manganese oxides that were formed during the coating process. Fig. 1(b) and (d) also showed manganese oxides formed in clusters, apparently on occupied surfaces. At the micron scale, the manganese-oxide-deposit obtained on each sorbent was composed of small particles on top of a more consolidated coating. The amount of manganese on the surface of the MOCS and MOCB, measured through acid digestion analysis, was approximately 1.5 mg Mn/g-sand and 2 mg Mn/g-crushed brick. It is to note that the quantity of manganese deposit obtained in this work for the two sorbents was found to be higher than that generally mentioned in the literature, which is about 0.003–0.5 mg Mn/g of sand [30,31]. This reflects the effectiveness of the coating process used in this study.

The elements associated with manganese-oxide-coatings were detected by the energy dispersive X-ray spectroscopy (EDAX) during SEM observations. It is to note that coated sorbents were dark colored, indicating the presence of manganese in the form of insoluble oxides. On the other hand, the X-ray diffraction patterns (XRD) of the two coated sorbents (data not shown) revealed that the manganese oxides were amorphous, since none specific diffraction ray indicative of any specific crystalline phase was detected.

The peak heights in the EDAX spectra are proportional to the metallic element concentrations (Fig. 2(a) and (b)). The EDAX spectra of MOCS (Fig. 2(a)) indicated that Mn, O, and Si are the main constituents. These had been expected to be the principal elements of MOCS. EDAX analysis yielded indirect evidence for the presence of manganese-oxide-coating on the surface of MOCS. The intense peak of Si occurring in EDAX spectrum showed that manganese oxides did

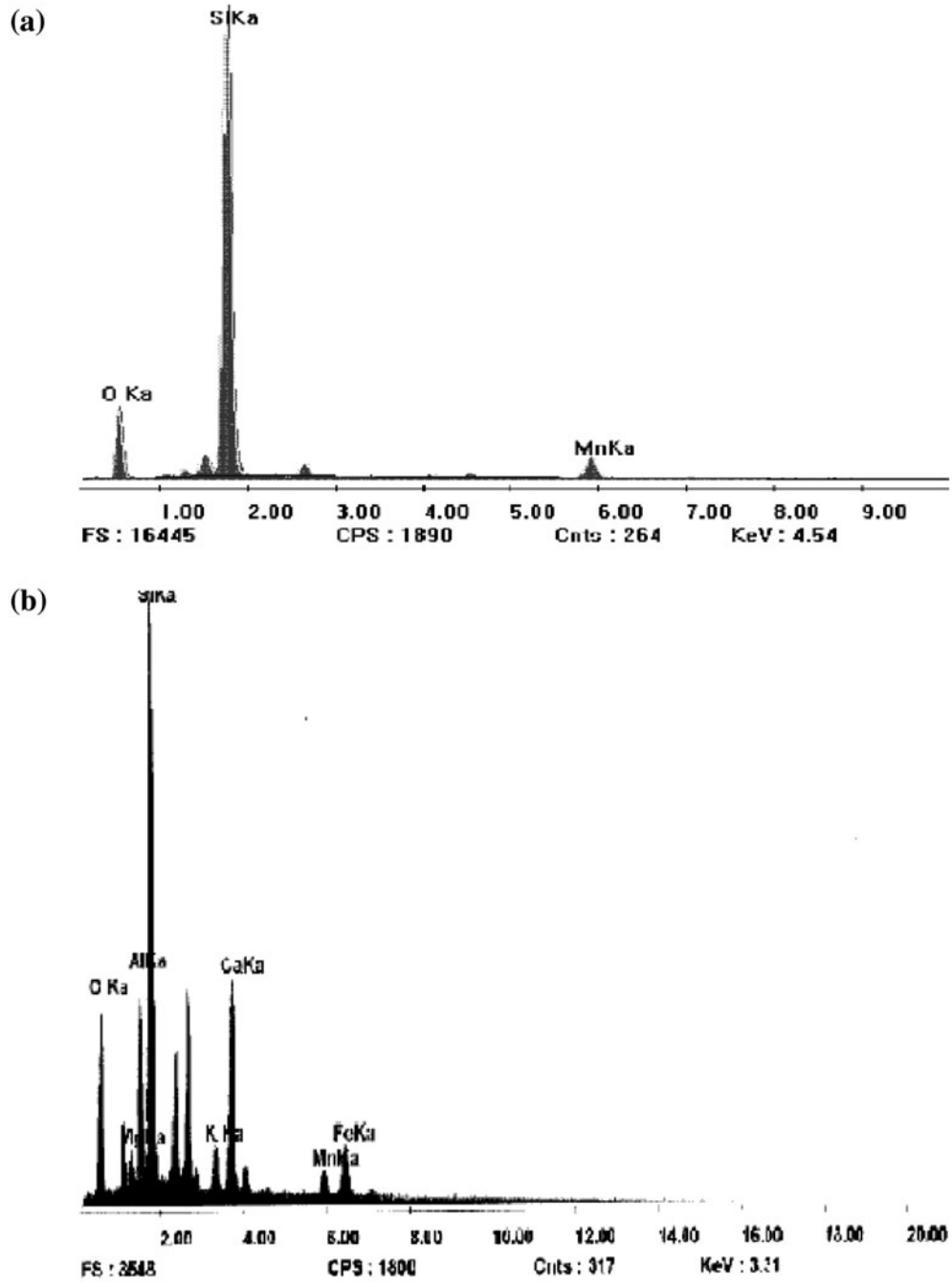

Fig. 2. EDAX spectrum of (a) MOCS and (b) MOCB.

not cover the full surface of the MOCS or that the coating was too thin, allowing the X-ray to reach the sand support. The EDAX spectrum of MOCB was illustrated in Fig. 2(b). It could be seen that Mn, O, Si, Al, Ca, and K are the dominant constituents. The presence of the Mn peak indicates the effectiveness of the adopted coating process.

3.1.2. Specific surface area

Results showed that specific surface areas of the two sorbents increased after coating. US and crushed brick had a surface area of 1.36 and 1.86 m^2/g, respectively. Surface coating with manganese oxide increased the surface area of sorbents to 3.81 and

4.64 m^2/g, respectively. This may be caused by the increase in both inner and surface porosity after adding the manganese oxides.

3.2. Batch adsorption experiments

3.2.1. Kinetic study

The effect of contact time on the sorption of phosphate ions (PO_4^{3-}) was studied for an initial concentration of 10 mg/l and a fixed pH solution of 5.0. The data showed that the sorption of phosphate ions on MOCB and MOCS was very fast at the initial stages of the contact period and thereafter it becomes slower near the equilibrium. Between these two stages of the uptake the rate of sorption is found to be nearly constant (Fig. 3). The differences in sorption capacities for the different sorbents can be related to the differences of their surface areas. In order to ensure that the equilibrium time was largely attained, subsequent experiments were carried out at a contact time of 2 h for all sorbents.

3.2.2. Effect of initial pH

When the initial pH of the solutions increases from 2.3 to 10.8, the removal of phosphate ions increases first and then decreases (Fig. 4). The maximum sorption capacity was observed at around pH 4. According to other works dealing with sorption of phosphate ions on hematite and Al_2O_3 [32], ion-exchange fiber [33], alunite [34], and bauxite [35], the removal decreases continuously for pH values ranging between around 4 and 10. The decrease in the phosphate ion uptake, occurring beyond pH5 (Fig. 4), implies probably a competition between phosphate ions and hydroxyl ions for the sorption on the surface Lewis acid sites of the sorbent. The effect of pH on phosphate adsorption can be explained also by considering a zero point of charge of the sorbent. Above the zero point of charge the positive charge density on the surface of the sorbents increases which disfavors the sorption of phosphate ions.

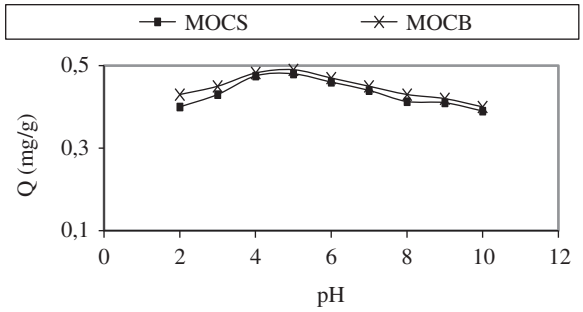

Fig. 4. Effect of initial pH on on PO_4^{3-} sorption on the two used sorbents, initial $[PO_4^{3-}] = 10$ mg/l.

The sorption of phosphate onto hydroxylated mineral surface can be described by a ligand exchange mechanism [36,37], which causes an increase in pH due to the hydroxyl ions released from the oxidic sorbent.

3.2.3. Retention of PO_4^{3-} by coated sorbents at 20°C

Phosphate ions sorption isotherms obtained for coating sorbents are shown in Fig. 5. These isotherms represent the sorption behavior of phosphate ions on the different sorbents as a function of increasing aqueous phosphate concentration for a contact time of 2 h.

The Freundlich isotherm model used for phosphate sorption (Fig. 6(a)) is the earliest known relationship describing the sorption equilibrium. The Freundlich isotherm constants obtained for the sorption of phosphate ions at 20°C on the different sorbents are mentioned in Table 1. The data showed that

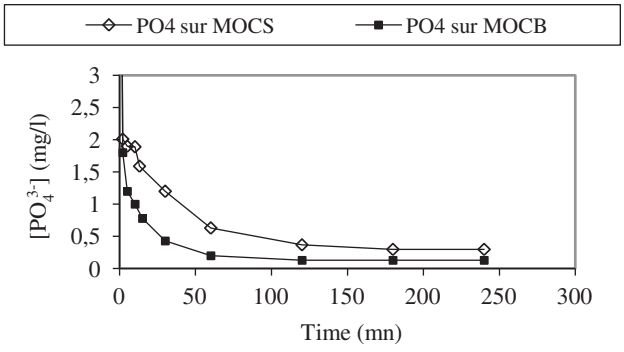

Fig. 3. Effect of contact time on PO_4^{3-} removal at pH 5 and at various PO_4^{3-} initial concentrations onto (a) MOCS and (b) MOCB.

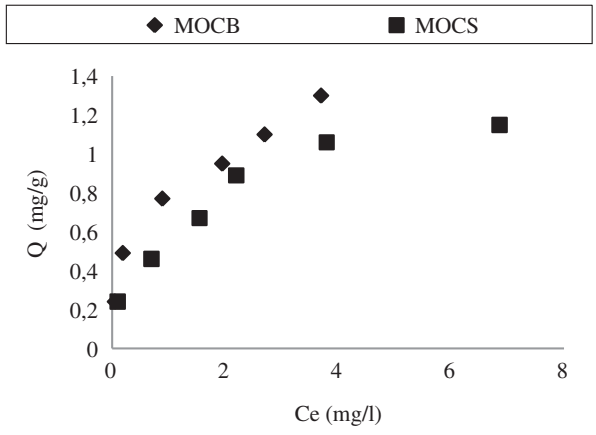

Fig. 5. Equilibrium isotherms at 20°C for PO_4^{3-} sorption on MOSC and MOCB.

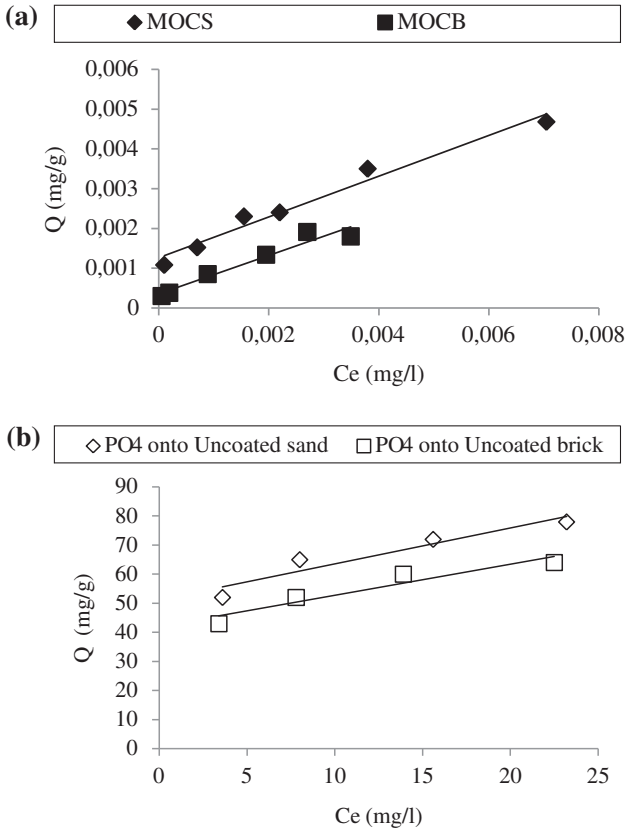

Fig. 6. Freundlich isotherms for the sorption of PO_4^{3-} at 20˚ C on MOCS and MOCB sorbent.

the K_F constant remained higher for coated crushed brick than for coated sand sorbent. Values obtained of $1 < n < 10$ imply favorable sorption of phosphate ions for the two sorbents [38]. The results of phosphate ion sorption onto MOCB and MOCS sorbents (Fig. 5) were also analyzed by using the Langmuir model to evaluate parameters associated with the sorption behavior. For the two sorbents, the sorption data fit to the linear form of the Langmuir equation (Fig. 7). This linear plot was employed to obtain the values of Q_0 and b from the slope and intercept of the plot (Table 1). The correlation coefficients (R^2) given in Table 1 show that the Langmuir equation gives also a fairly good fit to the sorption isotherms. Results in Table 1 show that Q_0 remains the highest for phosphate ion sorption onto coated crushed brick followed by coated sand, it is to note that capacity sorption onto uncoated sorbent (uncoated sand (US) and brick (UB)) were released and sorption capacities, determined by Langmuir model as shown in Fig. 6(b), were 0.82 and 0.93 mg/g for US and uncoated brick, respectively.

In order to compare the adsorption capacities of phosphate ion onto MOCB and MOCS sorbents, the adsorption capacities of various adsorbents are given in Table 2. Compared with most of the other adsorbents, the sorbents used in this study are comparable as qualitatively and it exhibited also a greater capacity for PO_4^{3-} adsorption (Table 2).

3.2.4. Adsorption thermodynamics

The calculated values of Gibbs free energy (ΔG°), enthalpy (ΔH°), and entropy (ΔS°) changes are given in Table 3. The negative values obtained for ΔG° indicate the spontaneous nature of sorption. Values of ΔH° and ΔS° were calculated from the slope and intercept of the Van't Hoff linear plot of log b vs. $1/T$ (Fig. 8). The positive of PO_4^{3-}.

3.3. Determination of kinetic parameters

To predict the sorption kinetics of phosphate ions onto the two sorbents, pseudo-first- and pseudo-second-order kinetic equations as well as intraparticle diffusion model were applied to experimental data relating to time-dependent PO_4^{3-} adsorption. Figs. 8 and 9 show the plots of linear forms of the three models for all the initial PO_4^{3-} concentrations considered. Kinetic parameters and correlation coefficients corresponding to the three models were calculated from these plots and listed in Table 4. As shown in this table, the R^2 values of the pseudo-second-order kinetic model are extremely high (>0.998) and are followed by those of the intraparticle diffusion equation and

Table 1
Freundlich and Langmuir constants ffor PO_4^{3-} sorption onto MOCS and MOCB

Temperature (˚C)	MOCS						MOCB					
	Langmuir constants			Freundlich constants			Langmuir constants			Freundlich constants		
	Q_0 (mg/g)	b (l/mg)	R^2	K_f	N	R^2	Q_0 (mg/g)	b (l/mg)	R^2	K_f	n	R^2
10	1.80	0.29	0.97	1.94	1.12	0.97	1.84	1.06	0.99	0.62	0.13	0.97
20	1.96	0.41	0.97	2.08	1.38	0.98	2.08	1.38	0.98	0.78	0.36	0.98
40	2.12	0.54	0.98	3.22	1.45	0.97	2.22	1.54	0.99	0.99	0.52	0.96

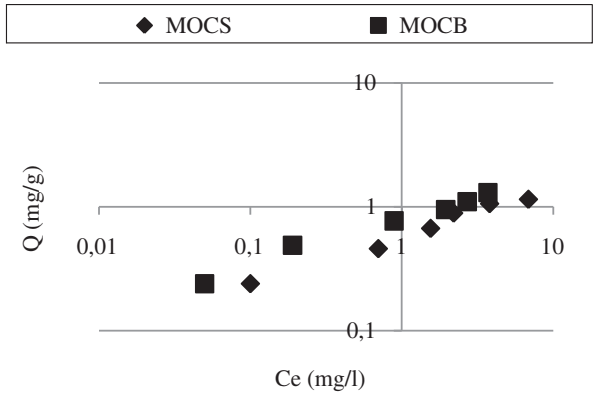

Fig. 7. Langmuir isotherms for the sorption of PO_4^{3-} at 20°C on MOCS and MOCB sorbent.

Table 2
Sorption capacity of PO_4^{3-} by various adsorbents

Adsorbents	Q_0 (mg/g)	Reference
MOCS	1.96	Present study
MOCB	2.08	Present study
Blast furnace slag	0.42	[39]
Black oxide	0.89	[40]
Shell sand	9.6	[41]
Red mud gypsum	5.07	[40]
Amorphous slag (I/II)	6.47	[42]

lastly by those of the pseudo first-order equation (Table 4). Moreover, the equilibrium phosphate uptakes (qe) deduced from the second-order correlation was much more reasonable—when compared with experimental results- than those of the first-order model. This suggests that the sorption process do not follow a pseudo-first-order reaction and the pseudo-second-order sorption kinetics seems to be predominant as shown in Fig. 10.

For the pseudo-second-order model, the rate constant K_2 and the initial sorption rate, h, decrease with increasing initial PO_4^{3-} concentration (Table 4). This suggests that the rate-limiting step may be a chemical adsorption [43]. The values of the rate constant K_2 from the pseudo-second-order model can be used to

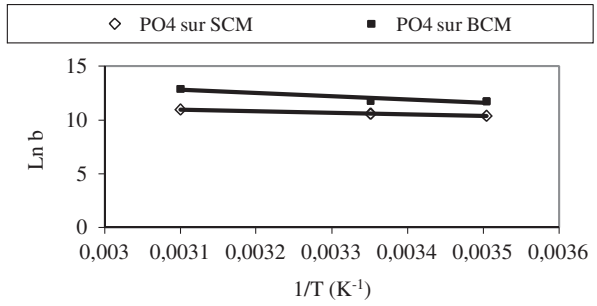

Fig. 8. Pseudo-first-order kinetic plots for the sorption of PO_4^{3-} ions onto (a) MOCS and (b) MOCB at various initial concentrations.

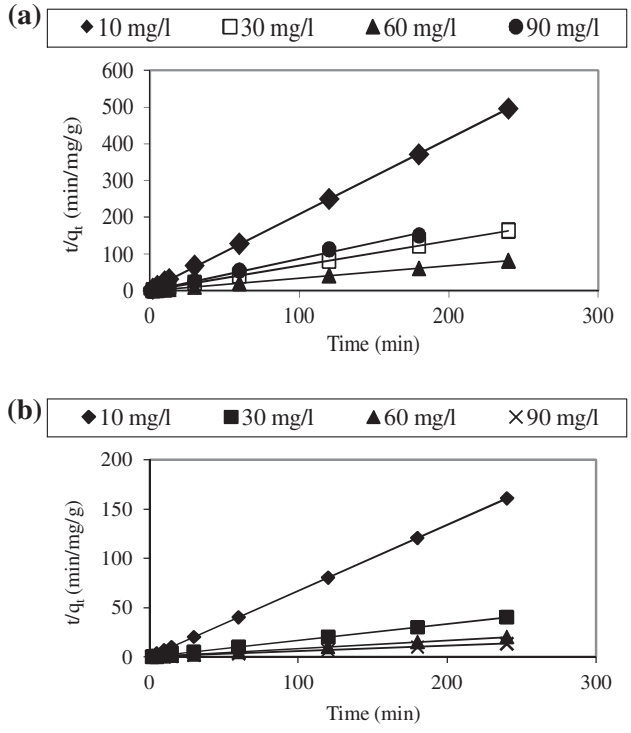

Fig. 9. Pseudo-second-order kinetic plots for the sorption of PO_4^{3-} ions onto (a) MOCS and (b) MOCB at various initial PO_4^{3-} concentrations.

calculate the activation energy of sorption process. The activation energy (E_a) was determined from the slope

Table 3
Thermodynamic parameters for the sorption of PO_4^{3-} onto MOCS and MOCB, at various temperatures

Temperature (°C)	MOCS			MOCB		
	ΔG° (kJ/mol)	ΔH° (kJ/mol)	ΔS° (kJ/(Kmol))	ΔG° (kJ/mol)	ΔH° (kJ/mol)	ΔS° (kJ/(Kmol))
10	−24.827	12.342	0.129	−2.703	24.693	0.182
20	−25.704	12.342	0.129	−28.862	24.693	0.182
40	−27.459	12.342	0.129	−30.640	24.693	0.182

Table 4
Kinetic parameters for the sorption of PO_4^{3-} onto MOCS and MOCB at various initial concentrations

Initial PO_4^{3-} concentration (mg/l)	MOCS						
	Pseudo-second-order kinetic model				Pseudo-first-order kinetic model		
	K_2 (g/mg.min)	$q_e \times 10^3$ (mg/g)	h (mg/g.min)	R^2	K_1 (min^{-1})	$q_e \times 10^3$ (mg/g)	R^2
10	1.35	0.48	0.31	0.99	0.345	56.23	0.69
30	0.81	1.49	1.81	1.00	0.029	37.15	0.61
60	0.71	1.61	1.85	0.99	0.021	1.27	0.74
90	0.66	2.94	5.73	0.99	0.016	0.38	0.86
MOCB							
10	2.85	1.49	6.32	0.99	0.018	75.5	0.77
30	1.66	5.98	59.36	0.99	0.011	11.72	0.70
60	0.75	17.85	103.45	0.99	0.0046	6.62	0.74
90	0.23	23.25	121.67	0.99	0.0023	4.28	0.66

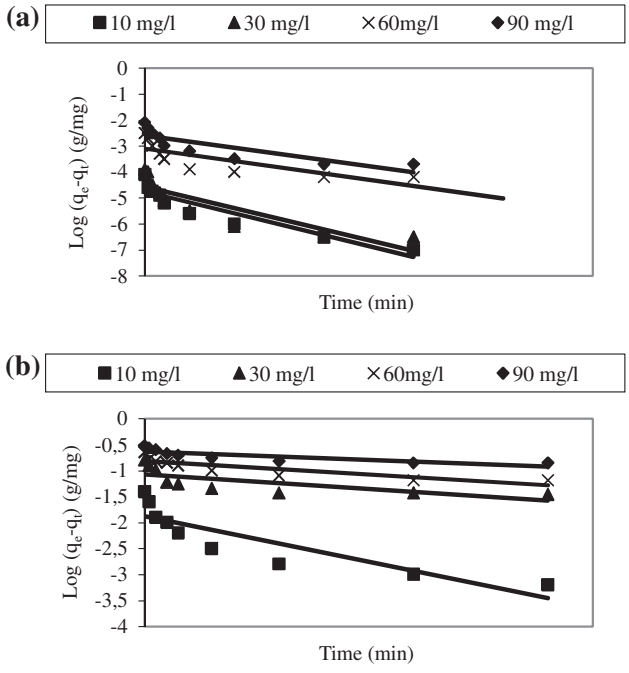

Fig. 10. Vant't Hoff plots for PO_4^{3-} sorption on the two sorbents.

of the Arrhenius plot of ln K_2 vs. 1/T (data not shown) according to Eq. (10). The values were found to be 8.01 and 12.62 kJ/mol for PO_4^{3-} sorption on MOCS and MOCB, respectively, showing that PO_4^{3-} sorption process by MOCS and MOCB is a nonactivated chemical adsorption, which confirm their chemical nature [44].

3.4. Sorption mechanism

According to previous work [45–47], inner-sphere complex is a complex formation where ligands replace water molecules from the inner coordination sphere and form bonds directly to the metal ion. In contrast, outer-sphere complex is another complex formation in which the ligand is situated with no bonds forming directly to the metal ion. It was founded that ions forming inner-sphere complexes show an increase or no variation in the adsorption capacity with increasing ionic strength. In contrast, ions forming outer-sphere surface complexes exhibit decreasing in the adsorption capacity with increasing solution ionic strength, which was formed mainly by electrostatic interactions and contain more than one water molecule between the adsorbate and the adsorbent functional groups. Therefore, the results obtained suggested the inner-sphere mechanism was mainly involved in the process of PO_4^{3-} adsorption in our study. Phosphate removal was mainly achieved by the replacement of surface hydroxyl groups by the phosphate species and formation of inner-sphere surface complexes at the water/oxide interface [48]. This can be attributed to the higher activity of the counter ions in the solution available to compensate the surface charge generated by specific ion adsorption [48].

4. Conclusion

Tow engineered sorbents: manganese-oxide-coated sand (MOCS) and crushed brick (MOCB) were prepared and characterized with regard to their morphology, mineralogy, and specific surface area. The results showed essentially that the deposited oxides were amorphous and correspond to 1.5 mg Mn/g-sand and 2 mg Mn/g-crushed brick. Moreover, surface coating with manganese-oxides considerably increased the surface area of the two sorbents.

Sorption of PO_4^{3-} ions onto MOCS and MOCB was studied considering the effect of initial pH as well as the thermodynamic and kinetic aspects of the sorption process. Data of sorption isotherms were correlated using Langmuir and Freundlich equations. The main conclusions that could be drawn from the whole results were as follows:

- the maximum of PO_4^{3-} sorption on the two sorbents took place at around pH 4;
- PO_4^{3-} sorption on the two sorbents followed a pseudo-second order reaction kinetics;
- values of activation energy, obtained for MOCS and MOCB from Arrhenius plots, suggested that the rate-limiting step of lead uptake might be a chemical adsorption;
- thermodynamic results indicated the spontaneous nature ($\Delta G^\circ < 0$) and the endothermic character ($\Delta H^\circ > 0$) of PO_4^{3-} sorption process.

Results from this study suggest that manganese-oxide-coated sorbents are potentially suitable to remove PO_4^{3-} ions from aqueous solution.

Acknowledgment

This research was financially supported by the Tunisian Chemical Group (SIAPE). The authors are highly thankful to Mr A. Charfi, Mr L. Fourati and Mme N. Ammar from the SIAPE for their assistance and their cooperation.

References

[1] L.E. De-Bashan, Y. Bashan, Recent advances in removing phosphorus from wastewater and its future use as fertilizer, Water Res. 38 (2004) 4222–4246.
[2] Y.A. Degs, M.A.M. Khraisheh, M.F. Tutunji, Sorption of lead ions on diatomite and manganese oxides modified diatomite, Water Res. 35 (2001) 3724–3728.
[3] E. Galarneau, R. Gehr, Phosphorus removal from wastewaters: Experimental and theoretical support for alternative mechanisms, Water Res. 31(2) (1997) 328–338.
[4] S.J. Shiao, K. Akashi, Phosphate removal from aqueous solutions using neutralised bauxite, J. WPCF 49(2) (1977) 280–285.
[5] E. Lopez, B. Soto, M. Arias, D. Rubinos, T. Barrel, Adsorbent properties of red mud and its use for wastewater treatment, Water Res. 32(4) (1998) 1314–1322.
[6] J. Pradhan, J. Das, S.N. Das, R.S. Thakur, Adsorption of phosphate from aqueous solution using activated red mud, J. Colloid Interface Sci. 204 (1998) 169–172.
[7] E. Oguz, Sorption of phosphate from solid/liquid interface by fly ash, Colloids Surf. A: Physicochem. Eng. Aspects 262 (1–3) (2005) 113–117.
[8] C.-H. Weng, C.P. Huang, Adsorption characteristics of Zn(II) from dilute aqueous solution by fly ash, Colloids Surf. A: Physicochem. Eng. Aspects 247 (2004) 137–143.
[9] J.A. Gomez del Rio, P.J. Morando, D.S. Cicerone, Natural materials for treatment of industrial effluents: Comparative study of the retention of Cd, Zn and Co by calcite and hydroxyapatite, Part I: Batch experiments, J. Environ. Manage. 71 (2004) 169–177.
[10] D. Buerge-Weirich, R. Hari, H. Xue, P. Behra, L. Sigg, Adsorption of Cu, Cd, and Ni on goethite in the presence of natural groundwater ligands, Environ. Sci. Technol. 36 (2002) 328–336.
[11] B.A. Manning, S.E. Fendorf, B. Bostick, D.L. Suarez, Arsenic (III) oxidation and adsorption reactions on synthetic birnessite, Environ. Sci. Technol. 36 (2002) 976–981.
[12] M.L. Kandah, Zinc and cadmium adsorption on low-grade phosphate, Sep. Purif. Technol. 35 (2004) 61–70.
[13] F.D. Tillman, S.L. Bartelt-Hunt, V.A. Craver, J.A. Smith, G.R. Alther, Relative metal ion sorption on natural and engineered sorbents: Batch and column studies, Environ. Eng. Sci. 22 (2005) 400–409.
[14] N.M. Agyei, C.A. Strydom, J.H. Potgieter, An investigation of phosphate ion adsorption from aqueous solution by fly ash and slag, Cem. Concr. Res. 30 (2000) 823–826.
[15] N.M. Agyei, C.A. Strydom, J.H. Potgieter, The removal of phosphate ions from aqueous solution by fly ash and slag, ordinary Portland cement and related blends, Cem. Concr. Res. 32(12) (2002) 1889–1897.
[16] G.M. Ayoub, B. Koopman, N. Pandya, Coated filter media for low concentration phosphorous removal, Water Environ. Res. 73 (2001) 478–485.
[17] J. Bouzid, Z. Elouear, M. Ksibi, M. Feki, A. Montiel, A study on removal characteristics of copper from aqueous solution by sewage sludge and pomace ashes, J. Hazard. Mater. 152 (2008) 838–845.
[18] R. Han, W. Zou, Z. Zhang, J. Shi, J. Yang, Removal of copper (II) and lead(II) from aqueous solution by manganese oxide coated sand: I. Characterization and kinetic study, J. Hazard. Mater. 137 (2006) 384–395.
[19] R. Han, W. Zou, H. Li, Y. Li, J. Shi, Copper(II) and lead(II) removal from aqueous solution in fixed-bed columns by manganese oxide coated zeolite, J. Hazard. Mater. 137 (2006) 934–942.
[20] M.K. Doula, Removal of Mn2+ ions from drinking water by using clinoptilolite and a clinoptilolite–Fe oxide system, Water Res. 40 (2006) 3167–3176.
[21] N. Boujelben, J. Bouzid, Z. Elouear, M. Feki, F. Jamoussi, A. Montiel, Removal of Mn2+ ions from drinking water by using clinoptilolite and a clinoptilolite–Fe oxide system, Water Res. 40 (2006) 3167–3176.
[22] V. Lenoble, O. Bouras, V. Deluchat, S. Serpaud, J.C. Bollinger, Arsenic adsorption onto pillared clays and iron oxides, J. Colloid Interface Sci. 225 (2002) 52–58.
[23] M. Walter, T. Arnold, T. Reich, G. Bernhard, Sorption of uranium(VI) onto ferric oxides in sulfate-rich acid waters, Environ. Sci. Technol. 37 (2003) 2898–2904.
[24] M.M. Benjamin, R.S. Slatten, R.P. Bailey, T. Bennett, Sorption and filtration of metals using iron oxide coated sand, Water Res. 30 (1996) 2609–2620.
[25] S.K. Sharma, B. Petrusevski, J.C. Schippers, Characterisation of coated sand from iron removal plants, J. Water Supply Res. Technol. 2 (2002) 247–257.
[26] M. Arienzo, P. Adamo, J. Chiarenzelli, M.R. Bianco, A.D. Martino, Retention of arsenic on hydrous ferric oxides generated by electrochemical peroxidation, Chemosphere 48 (2002) 1009–1018.
[27] S. Bajpai, M. Chaudhuri, Removal of arsenic from ground water by manganese dioxide coated sand, J. Env. Eng ASCE. 125 (1999) 782–784.
[28] S.L Lo, T. Jengh, C.H. Lai, Characteristics and adsorption properties of iron-coated sand, Water Sci. Technol. 35 (1997) 63–70.
[29] K.K. Panday, G. Prasad, V.N. Singh, Copper(II) removal from aqueous solutions by fly ash, Water Res. 19 (1985) 869–873.
[30] R. Selvaraj, K. Younghun, K.J. Cheol, Removal of copper from aqueous solution by aminated and protonated mesoporous aluminas: Kinetics and equilibrium, J. Colloid Interface Sci. 273 (2004) 14–21.

[31] Y.Y. Chang, K.S. Kim, J.H. Jung, J.K. Yang, S.M. Lee, Application of iron-coated sand and manganese-coated sand on the treatment of both As(III) and As(V), Water Sci. Technol. 55 (2007) 69–75.
[32] Po-Yu Hu, Yung-Hsu Hsieh, Jen-Ching Chen, Chen-Yu Chang, Characteristics of manganese-coated sand using SEM and EDAX analysis, J. Colloid Interface Sci. 274 (2004) 308–312.
[33] G. Horanyi, P. Joo, Some peculiarities in the specific adsorption of phosphate ions on hematite γ-Al_2O_3 as reflected by radiotracer studies, J. Colloid Interface Sci. 247 (2002) 12–17.
[34] L.R. Xia, G. Jinlong, T. Hongxiao, Adsorption of fluoride, phosphate, and arsenate ions on a new type of ion exchange fiber, J. Colloid Interface Sci. 248 (2002) 268–274.
[35] M. Ozacar, Phosphate adsorption characteristics of alunite to be used as a cement additive, Cem. Concr. Res. 2372 (2003) 1–5.
[36] H.S. Altundogan, F. Tumen, Removal of phosphates from aqueous solutions by using bauxite. I: Effect of pH on the adsorption of various phosphates, J. Chem. Tech. Biotechnol. 77 (2001) 77–85.
[37] S. Goldberg, G. Sposito, On the mechanism of specific phosphate adsorption by hydroxylated mineral surfaces: A review, Commun. Soil Sci. Plant Anal. 16 (1985) 801–821.
[38] G. Sposito, The Chemistry of Soils, Oxford University Press, New York, NY, 1989.
[39] R.A. Mann, H.J. Bavor, Phosphorus removal in constructed wetlands using gravel and industrial waste substrata, Water Sci. Technol. 27 (1993) 107–113.
[40] K.C. Cheung, T.H. Venkitachalam, W.D. Scott, Selecting soil amendment materials for removal of phosphorus, Water Sci. Technol. 30 (1994) 247–256.
[41] K. Ádám, A.K. Søvik, T. Krogstad, A. Heistad, Phosphorus removal by the fi lter materials light-weight aggregates and shell sand–A review of processes and experimental set-ups for improved design of fi lter systems for wastewater treatment, Vatten 63 (2007) 245–257.
[42] B. Kostura, H. Kulveitová, J. Lesko, Blast furnace slags as sorbents of phosphate from water solutions, Water Res. 39 (2005) 1795–1802.
[43] M. Arias, J. Da Silva-Carballal, L. Garcıa-Rıo, J. Mejuto, A. Nunez, Retention of phosphorus by iron and aluminum-oxides-coated quartz particles, J. Colloid Interface Sci. 295 (2006) 65–70.
[44] D.L. Sparks, Kinetics of Soil Chemical Processes, Academic Press, New York, NY, 1989.
[45] Ting Liua, Kun Wuc, Lihua Zeng, Removal of phosphorus by a composite metal oxide adsorbent derived from manganese ore tailings, J. Hazard. Mat. 217–218 (2012) 29–35.
[46] Z. Aksu, Determination of equilibrium. kinetic and thermodynamic parameters of the batch biosorption of nickel(II) ions onto Chlorella vulgaris, Process Biochem. 38 (2002) 89–99.
[47] G. Zhang, H. Liu, R. Liu, J. Qu, Removal of phosphate from water by a Fe–Mn binary oxide adsorbent, J. Colloid Interface Sci. 335 (2009) 168–174.
[48] S. Goldberg, C.T. Johnston, Mechanism of arsenic adsorption on amorphous oxides evaluated using macroscopic measurements, vibrational spectroscopy, and surface complexation modeling, J. Colloid Interface Sci. 234 (2001) 204–216.